JACS
JOURNAL OF THE AMERICAN CHEMICAL SOCIETY
Article
pubs.acs.org/JACS

High-Performance Electron Acceptor with Thienyl Side Chains for Organic Photovoltaics

Yuze Lin,[†,‡,§] Fuwen Zhao,[§] Qiao He,[†] Lijun Huo,[∥] Yang Wu,[⊥] Timothy C. Parker,[#] Wei Ma,[⊥] Yanming Sun,[∥] Chunru Wang,[§] Daoben Zhu,[§] Alan J. Heeger,[∥] Seth R. Marder,[#] and Xiaowei Zhan*[,†]

[†]Department of Materials Science and Engineering, College of Engineering, Key Laboratory of Polymer Chemistry and Physics of Ministry of Education, Peking University, Beijing 100871, China

[‡]Department of Chemistry, Capital Normal University, Beijing 100048, China

[§]Institute of Chemistry, Chinese Academy of Sciences, Beijing 100190, China

[∥]Heeger Beijing Research and Development Center, School of Chemistry and Environment, Beihang University, Beijing 100191, China

[⊥]State Key Laboratory for Mechanical Behavior of Materials, Xi'an Jiaotong University, Xi'an 710049, China

[#]School of Chemistry and Biochemistry and Center for Organic Photonics and Electronics, Georgia Institute of Technology, Atlanta, Georgia 30332-0400, United States

Supporting Information

ABSTRACT: We develop an efficient fused-ring electron acceptor (ITIC-Th) based on indacenodithieno[3,2-*b*]-thiophene core and thienyl side-chains for organic solar cells (OSCs). Relative to its counterpart with phenyl side-chains (ITIC), ITIC-Th shows lower energy levels (ITIC-Th: HOMO = −5.66 eV, LUMO = −3.93 eV; ITIC: HOMO = −5.48 eV, LUMO = −3.83 eV) due to the *σ*-inductive effect of thienyl side-chains, which can match with high-performance narrow-band-gap polymer donors and wide-band-gap polymer donors. ITIC-Th has higher electron mobility (6.1×10^{-4} cm^2 V^{-1} s^{-1}) than ITIC (2.6×10^{-4} cm^2 V^{-1} s^{-1}) due to enhanced intermolecular interaction induced by sulfur−sulfur interaction. We fabricate OSCs by blending ITIC-Th acceptor with two different low-band-gap and wide-band-gap polymer donors. In one case, a power conversion efficiency of 9.6% was observed, which rivals some of the highest efficiencies for single junction OSCs based on fullerene acceptors.

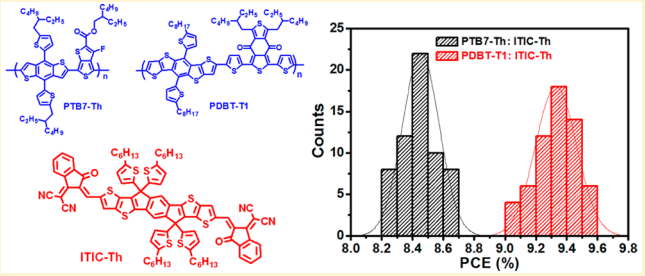

INTRODUCTION

Solar cells, which have the potential to be an inexpensive, renewable energy technology by efficiently converting sunlight into electricity, are promising long-term solutions for energy and environmental problems caused by mass production and use of fossil fuel, such as coal, oil, and gas. Significant research has been dedicated to the development of printable, flexible organic solar cells (OSCs) as a promising cost-effective, lightweight alternative to silicon-based solar cells for certain applications, such as the so-called bulk heterojunction architecture (BHJ)[1] in which typically a donor polymer (i.e., one with a low ionization energy) is blended with an acceptor (i.e., a material with a relatively high electron affinity). While many structures have been explored as donor polymers, and now several have yielded high-performance solar cells (> ∼7.5% efficiency and recently as high as 11%),[2−10] the vast majority of systems use a fullerene-based acceptor, in part because fullerenes exhibit relatively high electron affinity and isotropic charge transport properties.[1,11]

Recently some solution-processed, fullerene-free OSCs have shown greatly enhanced PCEs up to 6−8%,[12−25] which in several cases was even higher than those of the fullerene-based control devices. To date, the majority of nonfullerene acceptors (PCE > 6%) were constructed on the basis of a strategy of tailoring extended quasi-2D *π*-systems with electron-deficient groups like halogenated sub(na)phthalocyanine[26,27] and imide/diimide-functionalized rylenes.[12,14−17,28−33] In BHJ architectures with perylene diimides, care must be taken to find the correct balance for aggregation that leads to efficient charge separation and mobility, but not so much as to lead to complete phase separation. In light of these few examples, there is still much room to address the significant limitations of fullerene acceptors, specifically: they have relatively weak absorption in the visible and often constitute a large fraction of the material in the film; and they have relatively limited tunability of their electronic and optical properties. This provides both scientific and technological motivation to develop a general strategy for new acceptors, which can address these issues effectively. In an attempt to identify promising materials as nonfullerene

Received: February 23, 2016
Published: March 25, 2016

DOI: 10.1021/jacs.6b02004
J. Am. Chem. Soc. 2016, 138, 4955−4961

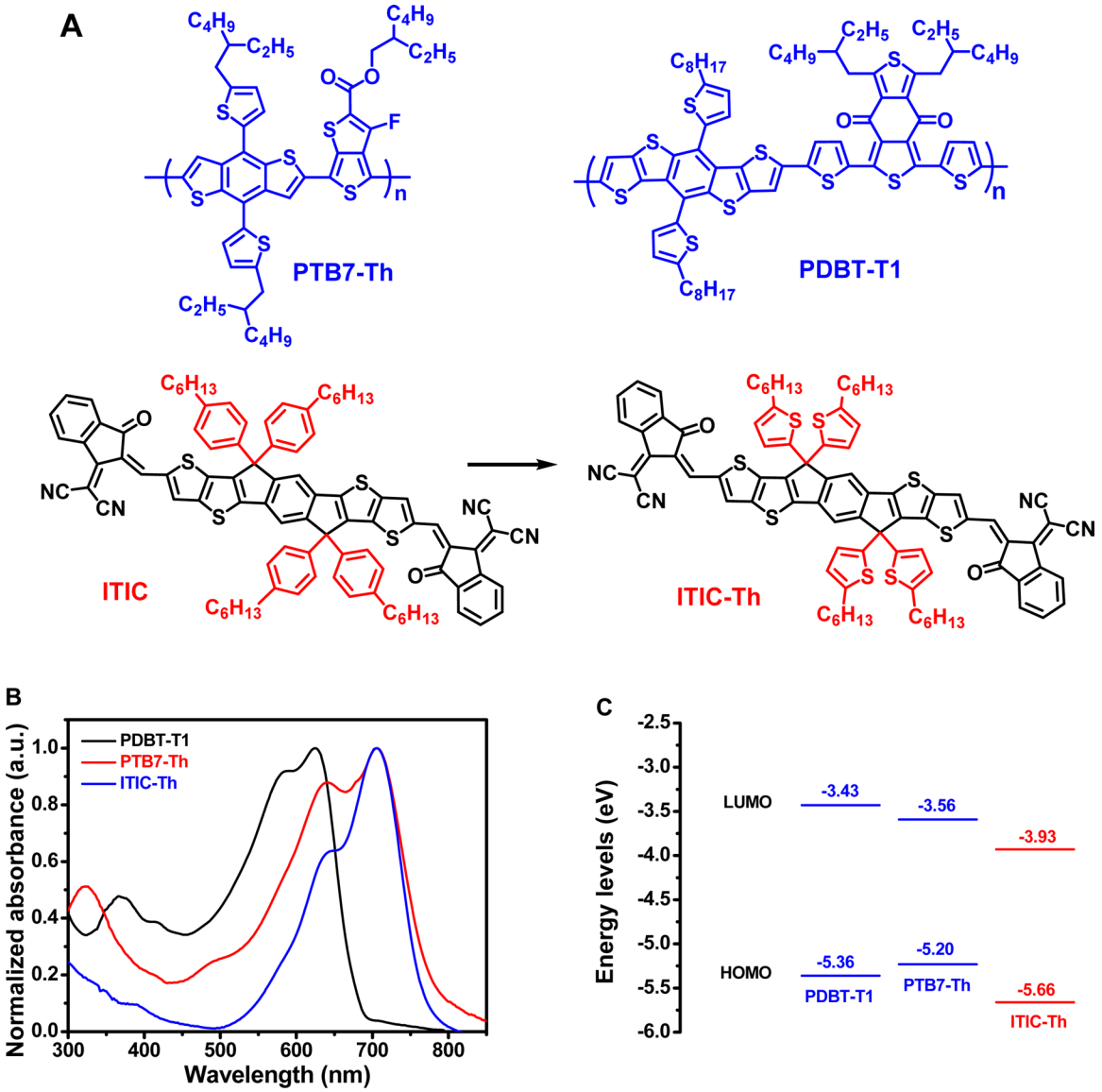

Figure 1. (A) Chemical structures of PTB7-Th, PDBT-T1, ITIC, and ITIC-Th. (B) UV−vis absorption spectra of PTB7-Th, PDBT-T1, and ITIC-Th in thin film. (C) Estimated energy levels of PTB7-Th, PDBT-T1, and ITIC-Th from electrochemical cyclic voltammetry.

acceptors, we proposed the following criteria as being important: (i) the basic properties, such as solubility, crystallinity, absorption, energy levels, and packing, can be varied somewhat systematically; (ii) the HOMO and LUMO levels that can be realized need to be appropriate for a range of donor polymers that are known to give high performance in solar cells; and (iii) the compounds should possess a rigid extended fused-ring backbone to decrease the reorganization energy and have wave functions in the LUMO that are delocalized to afford the opportunity for significant intermolecular electronic coupling, both of which are associated with high mobilities.

In the past for the most part as noted above, the structural building blocks for acceptors did not necessarily take full advantage of some of the design motifs that have led to high mobilities and absorptive properties of *donor* materials. We reasoned that use of the rigid indacenodithieno[3,2-*b*]-thiophene (IDTT) core subsitituted with strong electron-withdrawing groups could provide electron acceptor materials while providing out-of-plane side-chains[34] for tuning processability and morphology/phase separation. In our previous work, an electron acceptor (ITIC, Figure 1A) based on IDTT with four phenyl side-chains showed a promising PCE of 6.8%.[13] In ITIC, electron-withdrawing groups derived from 2-(3-oxo-2,3-dihydroinden-1-ylidene)malononitrile (shown in Scheme S1) lead to appropriate (and by use of modifications tunable) electron affinities (LUMO of ca. −3.83 eV).[13] Furthermore, acceptor−donor−acceptor structure in ITIC can induce intramolecular charge transfer and lead to both strong and somewhat panchromatic absorption throughout the visible (500−800 nm) relative to most fullerenes and even perylene dimides.[13] In addition, the four rigid substituents on IDTT main chain do not disrupt the planarity of the IDTT core, but may lead to low energetic dispersion identified by Sirringhaus and co-workers[35] to be impact for high mobilities (both hole and electron mobilities are $>10^{-2}$ cm^2 V^{-1} s^{-1}) in field-effect transistors.[36] However, ITIC possesses relatively high HOMO energy level of −5.48 eV, which leads to the limited compatibility with high-performance electron donors, especially moderate- or wide-band-gap donors with HOMO levels of ca.−

DOI: 10.1021/jacs.6b02004
J. Am. Chem. Soc. 2016, 138, 4955−4961

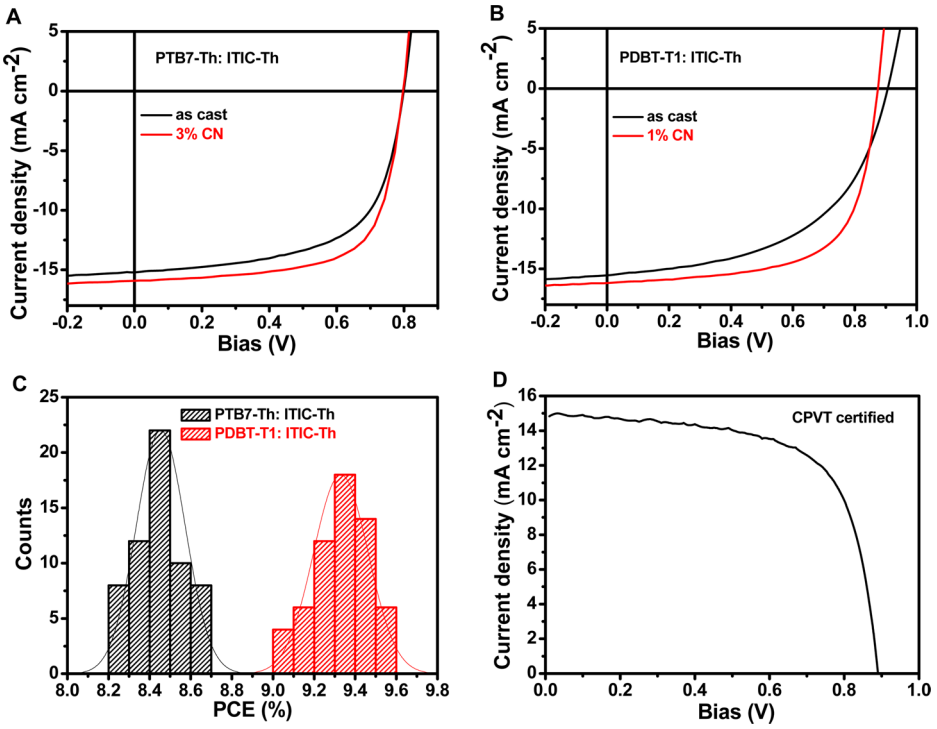

Figure 2. *J*–*V* curves of OSCs based on (A) PTB7-Th:ITIC-Th (1:1.3, w/w) and (B) PDBT-T1:ITIC-Th (1:1, w/w) without and with CN additive. (C) Statistical histogram of PCEs of OSCs based on PTB7-Th:ITIC-Th (1:1.3, w/w) and PDBT-T1:ITIC-Th (1:1, w/w) with CN (60 devices for each case). The average PCEs for PTB7-Th:ITIC-Th and PDBT-T1:ITIC-Th are 8.5% and 9.3%, respectively. (D) *J*–*V* curve of the OSCs based on PDBT-T1:ITIC-Th (1:1, w/w) with 1% CN certified by CPVT.

5.4 eV and even deeper, like PDBT-T1 (Figure 1A).[37] In addition, there is room for improvement in the electron mobility of ITIC (2.6×10^{-4} cm^2 V^{-1} s^{-1} measured by space-charge-limited current (SCLC) method), which is lower than those (10^{-3} cm^2 V^{-1} s^{-1}) of fullerene acceptors.

Here, we design and synthesize an electron acceptor (ITIC-Th, Figure 1A) based on IDTT as core and four 2-thienyl groups as out-of-plane side chains. Thienyl side-chains can downshift molecular energy levels relative to phenyl side-chains since 2-thienyl group is inductively somewhat electron-withdrawing.[38] As a result, ITIC-Th has lower energy levels, which can match with narrow-band-gap polymer donor like PTB7-Th (Figure 1A)[39] and wide-band-gap polymer donor like PDBT-T1.[37] Moreover, relative to phenyl side-chains, thienyl side-chains are expected to increase intermolecular interactions, which facilitate π-stacking and charge transport because the sulfur atoms are more easily polarized than carbon atoms of benzene and sulfur–sulfur interaction is stronger than carbon–carbon interaction. As a result, ITIC-Th has stronger absorption and higher electron mobility than ITIC. Finally, the PTB7-Th:ITIC-Th and PDBT-T1:ITIC-Th-based OSCs exhibited PCEs up to 8.7% and 9.6%, respectively, which are excellent values reported on OSCs based on new alternative acceptors. The 9.6% value is the highest PCE reported on the fullerene-free OSCs, and even higher than that of most of fullerene-based devices.

RESULTS AND DISCUSSION

Molecular Design and Characterization. ITIC-Th was synthesized by means of two facile reactions (Scheme S1). The indacenodithieno[3,2-*b*]thiophene with four thienyl side-chains (IT-Th) was lithiated and then quenched with dimethylformamide (DMF) to afford IT-CHO, followed by a Knoevenagel condensation with 2-(3-oxo-2,3-dihydroinden-1-ylidene)-malononitrile to afford ITIC-Th. Compound ITIC-Th has good solubility in common organic solvents (e.g., chloroform, *o*-dichlorobenzene (*o*-DCB)) and good thermal stability (5% weight loss at 310 °C in thermogravimetric analysis, Figure S1). ITIC-Th in dichloromethane solution (10^{-6} M) exhibits strong absorption in the 550–730 nm region with a maximum extinction coefficient of 1.5×10^5 M^{-1} cm^{-1} at 668 nm (Figure S2), which is slightly higher than that of ITIC in dichloromethane solution (1.3×10^5 M^{-1} cm^{-1} at 664 nm).[13] In comparison, the fullerene derivatives have very weak absorption in visible and near-infrared (NIR) region (for example, 6,6-phenyl C61 butyric acid methyl ester (PCBM), extinction coefficient < 1.4×10^3 M^{-1} cm^{-1} in 450–700 nm, see Figure S3). Relative to its solution, absorption of an ITIC-Th film exhibits a significant red-shift of 38 nm and a strong shoulder peak, suggesting that there is some molecular self-organization in the film. The optical band gap of ITIC-Th film estimated from the absorption edge (772 nm) is 1.60 eV (Figure 1B). The HOMO and LUMO energies of ITIC-Th film are estimated to be −5.66 and −3.93 eV (Figure 1C) from the onset oxidation and reduction potentials from electrochemical cyclic voltammetry (Figure S4), respectively. Due to the σ-inductive effect of thienyl side chains, ITIC-Th shows lower energy levels than those of ITIC (HOMO = −5.48 eV; LUMO = −3.83 eV).[13] In terms of thermodynamics, the energy levels of ITIC-Th can match with those of most typical electron donor materials (LUMO > −3.7 eV; HOMO > −5.4 eV). The electron mobility of ITIC-Th film measured using the space-charge-limited current (SCLC) method is up to 6.1×10^{-4} cm^2 V^{-1} s^{-1} (Figure S5) with an average value of 5.6×10^{-4} cm^2 V^{-1} s^{-1} for 10 devices, which is improved relative to that of ITIC (2.6×10^{-4} cm^2 V^{-1} s^{-1}) due to increased intermolecular

DOI: 10.1021/jacs.6b02004
J. Am. Chem. Soc. 2016, 138, 4955–4961

interactions in ITIC-Th. From grazing incident wide-angle X-ray diffraction (GIWAXS) analysis of ITIC and ITIC-Th neat films (Figure S6), ITIC-Th shows reduced *d*-spacing (ITIC-Th = 3.5 Å; ITIC = 3.8 Å) and increased coherence length (ITIC-Th = 5.5 nm; ITIC = 2.4 nm) of $\pi-\pi$ stacking relative to ITIC with phenyl side-chains. Then, this relatively high electron mobility is promising to ensure effective charge carrier transport to the electrodes.

Photovoltaic Performance. The LUMO of −3.59 eV and HOMO of −5.20 eV of electron donor PTB7-Th[18] are 0.34 and 0.46 eV higher than those of ITIC-Th (Figure 1C), respectively, and the LUMO and HOMO differences between PTB7-Th and ITIC-Th are expected to be sufficient for efficient exciton dissociation, for which a suggested empirical value of ca. 0.3 eV is often taken.[40] Thus, to demonstrate potential application of ITIC-Th in OSCs, we used PTB7-Th as a donor and ITIC-Th as an acceptor to fabricate BHJ OSCs with a structure of ITO/ZnO/PTB7-Th: ITIC-Th/MoO_x/Ag. Table S1 summarizes open circuit voltage (V_{OC}), short circuit current density (J_{SC}), fill factor (FF), and PCE of the devices at different donor/acceptor (D/A) weight ratios. OSCs based on as-cast PTB7-Th:ITIC-Th (1:1.3, w/w) film gave a V_{OC} of 0.80 V, J_{SC} of 15.15 mA cm^{-2}, FF of 0.618, and PCE of 7.5% (Figure 2A and Table 1). Furthermore, when 3% 1-chloronaphthalene (CN) was used, the OSC yielded an enhanced PCE of 8.7% (Figure 2A) with V_{OC} of 0.80 V, J_{SC} of 15.93 mA cm^{-2}, and FF of 0.680, and the average PCE value of 60 devices reached 8.5% (Figure 2C). As seen in Figure 1B, PTB7-Th shows strong absorption at 600−700 nm, which significantly overlaps with that of ITIC-Th. Our previously reported wide-band-gap (1.85 eV) polymer donor PDBT-T1 possesses complementary absorption (Figure 1B), suitable energy levels (HOMO = −5.36 eV; LUMO = −3.43 eV) matched with ITIC-Th (Figure 1C), and a high hole mobility of 0.03 cm^2 V^{-1} s^{-1}.[37] Thus, we used PDBT-T1 as a donor and ITIC-Th as an acceptor to fabricate BHJ OSCs. The devices processed from chloroform without any post-treatments show a PCE of 7.5% (Figure 2B, Tables 1 and S2). Similar to the case of the PTB7-Th:ITIC-Th system, CN can considerably improve the device performance of PDBT-T1:ITIC-Th. Relative to the devices as-cast, the devices with 1% CN additive show much higher FF, slightly higher J_{SC}, and finally higher PCE (9.6%, see Figure 2B, Tables 1 and S2). For 60 devices, the average PCE of PDBT-T1:ITIC-Th-based OSCs with 1% CN is 9.3% (Figure 2C), which is higher than those of other fullerene-free OSCs reported in literature. The devices without encapsulation were sent to the National Center of Supervision and Inspection on Solar Photovoltaic Products Quality of China (CPVT) for certification. A certified PCE of 8.85% was obtained with a J_{SC} of 15.01 mA cm^{-2}, V_{OC} of 0.89 V, and FF of 0.661 (Figures 2D and S7). The certified PCE value differs by 5% from the average value (9.3%) obtained from our laboratory. Among the parameters, the drop in efficiency results predominantly from the lower J_{SC}, most probably due to degradation of the device, because the devices were not encapsulated before testing at CPVT.

Table 1. Device Data of OSCs Based on PTB7-Th:ITIC-Th (1:1.3, w/w) and PDBT-T1:ITIC-Th (1:1, w/w) under the Illumination of AM 1.5 G, 100 mW cm^{-2}

donor	CN (%)	V_{OC} (V)	J_{SC} (mA cm^{-2})[a]	FF	PCE (%)[b]
PTB7-Th	0	0.80	15.15 (15.00)	0.618	7.5 (7.4)
	3	0.80	15.93 (15.95)	0.680	8.7 (8.5)
PDBT-T1	0	0.90	15.80 (15.75)	0.528	7.5 (7.4)
	1	0.88	16.24 (16.17)	0.671	9.6 (9.3)

[a]Values calculated from IPCE in brackets. [b]Average PCEs in brackets for 60 devices.

Compared with the PTB7-Th:ITIC-Th system, PDBT-T1:ITIC-Th-based devices show higher V_{OC} and J_{SC}; higher V_{OC} is related to lower HOMO of PDBT-T1, while higher J_{SC} is attributed to complementary absorption of PDBT-T1 and ITIC-Th, which is consistent with the incident photon to converted current efficiency (IPCE) spectra of the blended films (Figure S8). For both PTB7-Th:ITIC-Th and PDBT-T1:ITIC-Th, solvent additive CN improves the IPCE. Both PTB7-Th:ITIC-Th and PDBT-T1:ITIC-Th show the IPCE maximum up to ca. 80%. The highest J_{SC}'s of the devices based on PTB7-Th:ITIC-Th and PDBT-T1:ITIC-Th with CN calculated from integration of the IPCE spectra with the AM 1.5G reference spectrum are 15.95 and 16.17 mA cm^{-2}, respectively, which are very close to those measured by *J*−*V* measurements (15.93 and 16.24 mA cm^{-2}).

We investigate the initial stability of the best device of PDBT-T1:ITIC-Th-based OSCs (Figure S9). After heating at 100 °C for 5−10 min, the device PCE decreases ca. 10%, and then keeps almost stable around 85−88% of original value. In contrast, the PCE of PDBT-T1:PCBM-based device decreases 35% after heating at 100 °C for 3 h. Furthermore, PDBT-T1:ITIC-Th-based OSCs also show better long-term stability than PDBT-T1:PCBM-based OSCs under storage at room temperature both in N_2 glovebox and in ambient condition.

Film Morphology Analysis. To better understand the role of the solvent additive CN, the morphology of PTB7-Th or PDBT-T1:ITIC-Th blended films was investigated. From atomic force microscopy (AFM) images (Figures S10 and S11), the PTB7-Th:ITIC-Th and PDBT-T1:ITIC-Th blended films show relatively smooth surfaces. GIWAXS was used to investigate the molecular-level structural information such as molecular orientation and packing of PTB7-Th:ITIC-Th and PDBT-T1:ITIC-Th with and without CN solvent additive. The two-dimensional (2D) GIWAXS patterns of blends with or without CN are shown in Figure 3A, and the corresponding scattering profiles in the in-plane and out-of-plane direction are displayed in Figure 3B. The peaks with $q \approx 0.3$ and 0.9 Å^{-1} are generated from the lamellar packing of PTB7-Th or PDBT-T1 (the scattering of the corresponding neat films is shown in Figure S12). The sharp peaks with $q \approx 0.48$ and 0.96 Å^{-1} originate from ITIC-Th lamellar packing (Figure S12). The $\pi-\pi$ stacking peak of PTB7-Th and PDBT-T1 is shown at $q \approx$ 1.6−1.7 Å^{-1}. It is interesting to note that all the peaks become sharper/stronger after processed with additive CN, which indicates that CN enhances molecular packing of both conjugated donor polymers (PTB7-Th and PDBT-T1) and ITIC-Th in the blended film. The coherence length of PTB7-Th and ITIC-Th $\pi-\pi$ stacking is calculated (via Scherrer equation)[41] to be 1.4, 3.0 nm and 1.5, 3.8 nm for the blend without and with CN, respectively. The coherence length of PDBT-T1 and ITIC-Th $\pi-\pi$ stacking is calculated to be 1.2, 2.8 nm and 1.3, 3.3 nm for the blend without and with CN, respectively. This again confirms that the molecular packing is improved after processing with CN, which may be attributed to different solubility of donor and acceptor in CN (~40 mg mL^{-1} for ITIC-Th, ~9 mg mL^{-1} for PTB7-Th, ~0.5 mg mL^{-1} for PDBT-T1) and different drying speed of solution (boiling

DOI: 10.1021/jacs.6b02004
J. Am. Chem. Soc. 2016, 138, 4955−4961

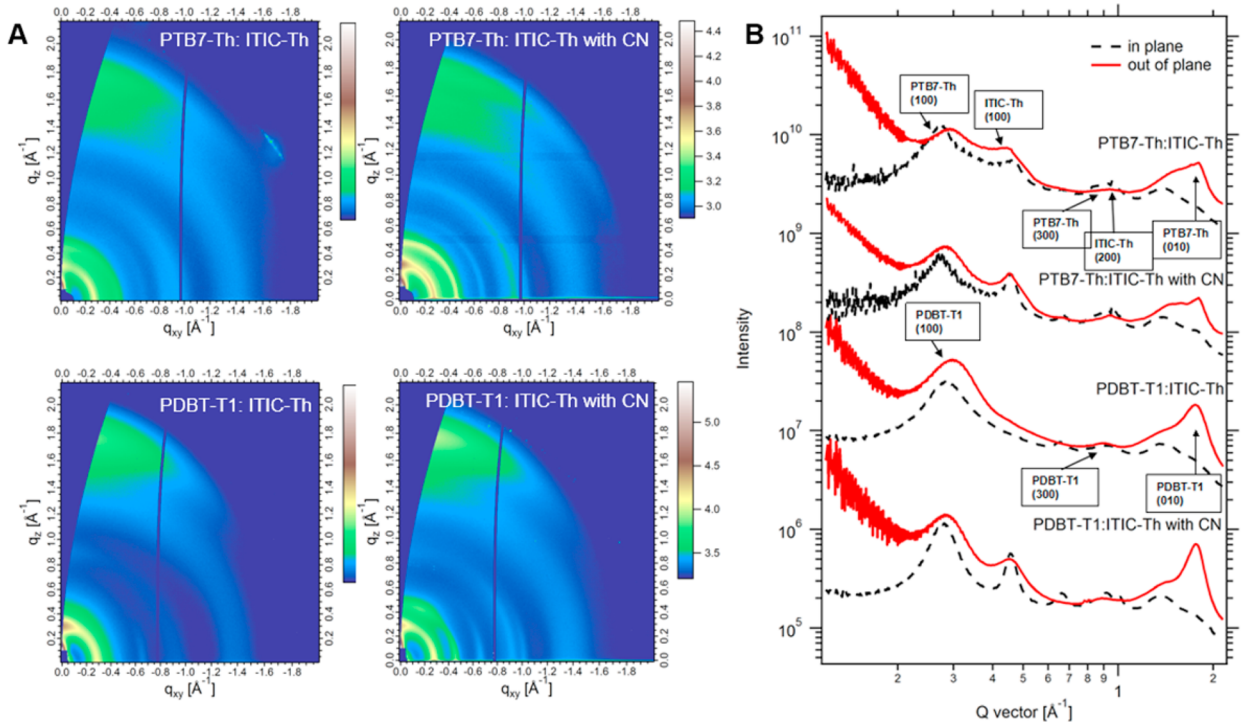

Figure 3. (A) 2D GIWAXS patterns and (B) scattering profiles of in-plane and out-of-plane for PTB7-Th:ITIC-Th (1:1.3, w/w) and PDBT-T1:ITIC-Th (1:1, w/w) blended films as-spun and processed with CN (3% for PTB7-Th:ITIC-Th, 1% for PDBT-T1:ITIC-Th).

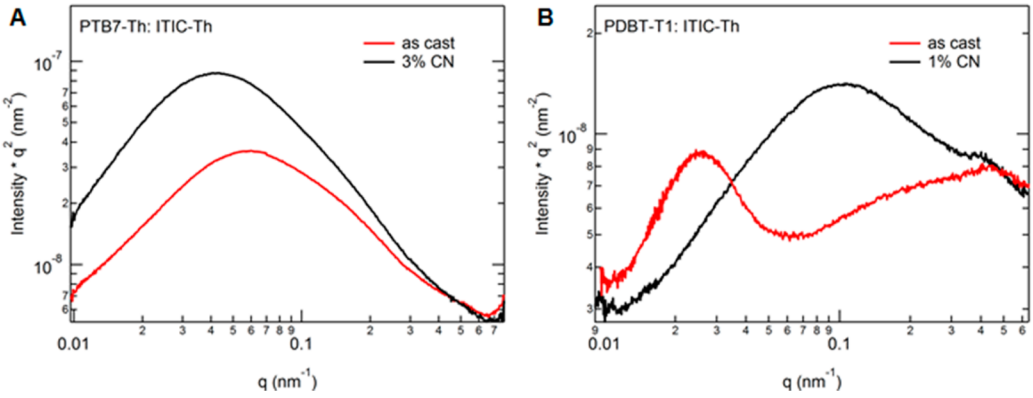

Figure 4. R-SoXS profiles in log scale for (A) PTB7-Th:ITIC-Th (1:1.3, w/w) blended films without and with 3% CN additive and (B) PDBT-T1:ITIC-Th (1:1, w/w) blended films without and with 1% CN additive.

point of CN, *o*-DCB and chloroform is ~260, 180 and 61 °C, respectively). The improved $\pi-\pi$ stacking ordering will be favorable for charge transport and thus device performance. Also, the $\pi-\pi$ stacking in the out-of-plane direction of blended films processed without and with CN is obviously stronger than those in the in-plane direction, which indicates molecules take predominantly face-on orientation relative to the electrode substrates. The vertical $\pi-\pi$ stacking is well-known to benefit charge transport between anode and cathode of solar cells.

In addition, resonant soft X-ray scattering (R-SoXS) was used to probe the phase separation in PTB7-Th or PDBT-T1:ITIC-Th blended films (Figure 4). The resonant energy 284.8 eV was selected to provide highly enhanced contrast.[41] The median of the distribution s_{median} of the scattering corresponds to the characteristic median length scale, ξ, of the corresponding log-normal distribution in real space with $\xi = 1/s_{median}$, a model independent statistical quantity. It is noted that the median domain size is the half of ξ. The ξ of 60−70 nm is obtained for the PTB7-Th:ITIC-Th blends without any treatment. Further analysis reveals that PTB7-Th:ITIC-Th films with 3% CN show slightly larger phase separation with ξ of 90−100 nm. Furthermore, R-SoXS can also reveal the average composition variations (relative domain purity) via integrating scattering profiles, which are indicative of the average purity of donor material and acceptor material domains. In Figure 4, the higher the total scattering intensity (integration of the scattering profiles over q), the purer the average domains. The relative domain purity of the as-cast blend is about 82% of the blend processed with CN. Thus, 3% CN increases average domain purity of the film. The purer domains are favorable to reduce bimolecular recombination.[42] Meanwhile, in the PDBT-T1: ITIC-Th system, we can find that PDBT-T1:ITIC-Th films with 1% CN shows smaller $\xi \sim 50$ nm than that of the blend film without CN ($\xi \sim 200$ nm). The total scattering intensity of PDBT-T1:ITIC-Th without CN is lower than that with the addition of 1% CN, which indicates that CN leads to higher

DOI: 10.1021/jacs.6b02004
J. Am. Chem. Soc. 2016, 138, 4955−4961

relative domain purity. The appropriate domain sizes and the pure domains are beneficial to exciton dissociation and charge transport, respectively.[43] As a result, the PTB7-Th:ITIC-Th and PDBT-T1:ITIC-Th with CN show higher J_{SC} and FF, and finally higher PCE.

PTB7-Th or PDBT-T1: ITIC-Th blended films without and with CN as solvent additive show balanced charge transport (electron mobility/hole mobility = 1.3−2.2, Table S3), with relatively high hole and electron mobilities in order of magnitude of 10^{-4} cm^2 V^{-1} s^{-1} (Table S3, Figures S13−S16). As GIWAXS and R-SoXS predicted, for both PTB7-Th:ITIC-Th and PDBT-T1:ITIC-Th systems, the blended films with CN exhibit higher hole and electron mobilities than as-cast films, due to the improved $\pi-\pi$ stacking ordering (see in GIWAXS analysis) and higher domain purity (see in R-SoXS analysis) in the blended films. Thus, in these two systems, CN improves J_{SC}, FF, and PCE.

CONCLUSIONS

ITIC-Th with thienyl side-chains exhibits relatively stronger absorption in the visible and NIR regions, lower energy levels, and higher electron mobility relative to ITIC with phenyl side-chains. PTB7-Th:ITIC-Th and PDBT-T1:ITIC-Th blended film show balanced charge transport and predominant intermolecular $\pi-\pi$ interactions vertical to the substrates. The solvent additive CN improves the phase purity and charge transport of blended film. The OSCs based on PTB7-Th:ITIC-Th blended films with 3% CN show PCEs as high as 8.7%. Furthermore, relative to narrow-band-gap PTB7-Th, the wide-band-gap polymer donor PDBT-T1 has a lower HOMO energy level and more complementary absorption with ITIC-Th; PDBT-T1:ITIC-Th-based devices with 1% CN show PCEs as high as 9.6%, with an average PCE of 9.3% and a certified PCE of 8.85%, which are higher than those (6−8%) reported on fullerene-free OSCs. We expect that the PCE could be further enhanced to breaking 10% after careful device optimization, such as cathode/anode interlayers and plasmonic nanostructures. These results demonstrate that the approach we described above, clearly illustrated with the electron acceptor ITIC-Th, is a promising alternative to those based on fullerene (or rylene diimide) derivatives for high-performance OSCs, and we suggest that this approach can be broadly applicable to the development of new acceptors for a wide range of donor materials given the tunability of the building blocks and the modularity of the synthetic strategy.

ASSOCIATED CONTENT

Supporting Information

The Supporting Information is available free of charge on the ACS Publications website at DOI: 10.1021/jacs.6b02004.

Detailed experimental procedures including synthesis, characterization and device fabrication, and additional characterization data, such as CV, SCLC, AFM and GIWAXS (PDF)

AUTHOR INFORMATION

Corresponding Author

*xwzhan@pku.edu.cn

Notes

The authors declare no competing financial interest.

ACKNOWLEDGMENTS

X.Z. thanks the 973 Program (No. 2013CB834702) and the NSFC (No. 91433114, 51261130582). Y.L. thanks the NSFC (No. 21504058). W.M. thanks the NSFC (No. 21504006). L.H. and Y.S. thank the International Science & Technology Cooperation Program of China (2014DFA52820) and the 111 project (B14009). X-ray data was acquired at beamline 11.0.1.2 and 7.3.3 at the Advanced Light Source, which is supported by the Director, Office of Science, Office of Basic Energy Sciences, of the U.S. Department of Energy under Contract No. DE-AC02-05CH11231. S.R.M., T.C.P. and A.J.H. thank Department of the Navy, Office of Naval Research Award No. N00014-14-1-0580.

REFERENCES

(1) Yu, G.; Gao, J.; Hummelen, J. C.; Wudl, F.; Heeger, A. J. *Science* **1995**, *270*, 1789.
(2) Page, Z. A.; Liu, Y.; Duzhko, V. V.; Russell, T. P.; Emrick, T. *Science* **2014**, *346*, 441.
(3) Kim, J. Y.; Lee, K.; Coates, N. E.; Moses, D.; Nguyen, T. Q.; Dante, M.; Heeger, A. J. *Science* **2007**, *317*, 222.
(4) Zhou, Y. H.; Fuentes-Hernandez, C.; Shim, J.; Meyer, J.; Giordano, A. J.; Li, H.; Winget, P.; Papadopoulos, T.; Cheun, H.; Kim, J.; Fenoll, M.; Dindar, A.; Haske, W.; Najafabadi, E.; Khan, T. M.; Sojoudi, H.; Barlow, S.; Graham, S.; Bredas, J. L.; Marder, S. R.; Kahn, A.; Kippelen, B. *Science* **2012**, *336*, 327.
(5) Liu, Y. H.; Zhao, J. B.; Li, Z. K.; Mu, C.; Ma, W.; Hu, H. W.; Jiang, K.; Lin, H. R.; Ade, H.; Yan, H. *Nat. Commun.* **2014**, *5*, 5293.
(6) You, J. B.; Dou, L. T.; Yoshimura, K.; Kato, T.; Ohya, K.; Moriarty, T.; Emery, K.; Chen, C. C.; Gao, J.; Li, G.; Yang, Y. *Nat. Commun.* **2013**, *4*, 1446.
(7) Ouyang, X.; Peng, R.; Ai, L.; Zhang, X.; Ge, Z. *Nat. Photonics* **2015**, *9*, 520.
(8) Lu, L.; Kelly, M. A.; You, W.; Yu, L. *Nat. Photonics* **2015**, *9*, 491.
(9) Huo, L.; Liu, T.; Sun, X.; Cai, Y.; Heeger, A. J.; Sun, Y. *Adv. Mater.* **2015**, *27*, 2938.
(10) Guo, X. G.; Zhou, N. J.; Lou, S. J.; Smith, J.; Tice, D. B.; Hennek, J. W.; Ortiz, R. P.; Navarrete, J. T. L.; Li, S. Y.; Strzalka, J.; Chen, L. X.; Chang, R. P. H.; Facchetti, A.; Marks, T. J. *Nat. Photonics* **2013**, *7*, 825.
(11) Sariciftci, N. S.; Smilowitz, L.; Heeger, A. J.; Wudl, F. *Science* **1992**, *258*, 1474.
(12) Zhong, Y.; Trinh, M. T.; Chen, R.; Purdum, G. E.; Khlyabich, P. P.; Sezen, M.; Oh, S.; Zhu, H.; Fowler, B.; Zhang, B.; Wang, W.; Nam, C.-Y.; Sfeir, M. Y.; Black, C. T.; Steigerwald, M. L.; Loo, Y.-L.; Ng, F.; Zhu, X. Y.; Nuckolls, C. *Nat. Commun.* **2015**, *6*, 8242.
(13) Lin, Y. Z.; Wang, J. Y.; Zhang, Z. G.; Bai, H. T.; Li, Y. F.; Zhu, D. B.; Zhan, X. W. *Adv. Mater.* **2015**, *27*, 1170.
(14) Hwang, Y.-J.; Li, H.; Courtright, B. A. E.; Subramaniyan, S.; Jenekhe, S. A. *Adv. Mater.* **2016**, *28*, 124.
(15) Jung, J. W.; Jo, J. W.; Chueh, C. C.; Liu, F.; Jo, W. H.; Russell, T. P.; Jen, A. K. Y. *Adv. Mater.* **2015**, *27*, 3310.
(16) Hwang, Y.-J.; Courtright, B. A. E.; Ferreira, A. S.; Tolbert, S. H.; Jenekhe, S. A. *Adv. Mater.* **2015**, *27*, 4578.
(17) Sun, D.; Meng, D.; Cai, Y.; Fan, B.; Li, Y.; Jiang, W.; Huo, L.; Sun, Y.; Wang, Z. *J. Am. Chem. Soc.* **2015**, *137*, 11156.
(18) Lin, Y. Z.; Zhang, Z. G.; Bai, H. T.; Wang, J. Y.; Yao, Y. H.; Li, Y. F.; Zhu, D. B.; Zhan, X. W. *Energy Environ. Sci.* **2015**, *8*, 610.
(19) Kim, T.; Kim, J.-H.; Kang, T. E.; Lee, C.; Kang, H.; Shin, M.; Wang, C.; Ma, B.; Jeong, U.; Kim, T.-S.; Kim, B. J. *Nat. Commun.* **2015**, *6*, 8547.
(20) Lin, H.; Chen, S.; Li, Z.; Lai, J. Y. L.; Yang, G.; McAfee, T.; Jiang, K.; Li, Y.; Liu, Y.; Hu, H.; Zhao, J.; Ma, W.; Ade, H.; Yan, H. *Adv. Mater.* **2015**, *27*, 7299.
(21) Gao, L.; Zhang, Z.-G.; Xue, L.; Min, J.; Zhang, J.; Wei, Z.; Li, Y. *Adv. Mater.* **2016**, *28*, 1884.

DOI: 10.1021/jacs.6b02004
J. Am. Chem. Soc. 2016, 138, 4955−4961

(22) Meng, D.; Sun, D.; Zhong, C.; Liu, T.; Fan, B.; Huo, L.; Li, Y.; Jiang, W.; Choi, H.; Kim, T.; Kim, J. Y.; Sun, Y.; Wang, Z.; Heeger, A. J. *J. Am. Chem. Soc.* **2016**, *138*, 375.
(23) Lin, Y. Z.; He, Q.; Zhao, F. W.; Huo, L. J.; Mai, J. Q.; Lu, X. H.; Su, C. J.; Li, T. F.; Wang, J. Y.; Zhu, J. S.; Sun, Y. M.; Wang, C. R.; Zhan, X. W. *J. Am. Chem. Soc.* **2016**, *138*, 2973.
(24) Kwon, O. K.; Uddin, M. A.; Park, J.-H.; Park, S. K.; Nguyen, T. L.; Woo, H. Y.; Park, S. Y. *Adv. Mater.* **2016**, *28*, 910.
(25) Nielsen, C. B.; Holliday, S.; Chen, H.-Y.; Cryer, S. J.; McCulloch, I. *Acc. Chem. Res.* **2015**, *48*, 2803.
(26) Cnops, K.; Rand, B. P.; Cheyns, D.; Verreet, B.; Empl, M. A.; Heremans, P. *Nat. Commun.* **2014**, *5*, 3406.
(27) Cnops, K.; Zango, G.; Genoe, J.; Heremans, P.; Martinez-Diaz, M. V.; Torres, T.; Cheyns, D. *J. Am. Chem. Soc.* **2015**, *137*, 8991.
(28) Zhan, X.; Tan, Z. a.; Domercq, B.; An, Z.; Zhang, X.; Barlow, S.; Li, Y.; Zhu, D.; Kippelen, B.; Marder, S. R. *J. Am. Chem. Soc.* **2007**, *129*, 7246.
(29) Pho, T. V.; Toma, F. M.; Chabinyc, M. L.; Wudl, F. *Angew. Chem., Int. Ed.* **2013**, *52*, 1446.
(30) Hartnett, P. E.; Timalsina, A.; Matte, H. S. S. R.; Zhou, N.; Guo, X.; Zhao, W.; Facchetti, A.; Chang, R. P. H.; Hersam, M. C.; Wasielewski, M. R.; Marks, T. J. *J. Am. Chem. Soc.* **2014**, *136*, 16345.
(31) Mu, C.; Liu, P.; Ma, W.; Jiang, K.; Zhao, J. B.; Zhang, K.; Chen, Z. H.; Wei, Z. H.; Yi, Y.; Wang, J. N.; Yang, S. H.; Huang, F.; Facchetti, A.; Ade, H.; Yan, H. *Adv. Mater.* **2014**, *26*, 7224.
(32) Schmidt-Mende, L.; Fechtenkotter, A.; Mullen, K.; Moons, E.; Friend, R. H.; MacKenzie, J. D. *Science* **2001**, *293*, 1119.
(33) Diao, Y.; Zhou, Y.; Kurosawa, T.; Shaw, L.; Wang, C.; Park, S.; Guo, Y.; Reinspach, J. A.; Gu, K.; Gu, X.; Tee, B. C.; Pang, C.; Yan, H.; Zhao, D.; Toney, M. F.; Mannsfeld, S. C.; Bao, Z. *Nat. Commun.* **2015**, *6*, 7955.
(34) Mei, J. G.; Bao, Z. N. *Chem. Mater.* **2014**, *26*, 604.
(35) Venkateshvaran, D.; Nikolka, M.; Sadhanala, A.; Lemaur, V.; Zelazny, M.; Kepa, M.; Hurhangee, M.; Kronemeijer, A. J.; Pecunia, V.; Nasrallah, I.; Romanov, I.; Broch, K.; McCulloch, I.; Emin, D.; Olivier, Y.; Cornil, J.; Beljonne, D.; Sirringhaus, H. *Nature* **2014**, *515*, 384.
(36) Xu, Y.-X.; Chueh, C.-C.; Yip, H.-L.; Ding, F.-Z.; Li, Y.-X.; Li, C.-Z.; Li, X.; Chen, W.-C.; Jen, A. K. Y. *Adv. Mater.* **2012**, *24*, 6356.
(37) Huo, L.; Liu, T.; Sun, X.; Cai, Y.; Heeger, A. J.; Sun, Y. *Adv. Mater.* **2015**, *27*, 2938.
(38) Zhan, X.; Risko, C.; Amy, F.; Chan, C.; Zhao, W.; Barlow, S.; Kahn, A.; Brédas, J.-L.; Marder, S. R. *J. Am. Chem. Soc.* **2005**, *127*, 9021.
(39) Liao, S. H.; Jhuo, H. J.; Cheng, Y. S.; Chen, S. A. *Adv. Mater.* **2013**, *25*, 4766.
(40) Veldman, D.; Meskers, S. C. J.; Janssen, R. A. J. *Adv. Funct. Mater.* **2009**, *19*, 1939.
(41) Smilgies, D. M. *J. Appl. Crystallogr.* **2013**, *46*, 286.
(42) Ma, W.; Tumbleston, J. R.; Wang, M.; Gann, E.; Huang, F.; Ade, H. *Adv. Energy Mater.* **2013**, *3*, 864.
(43) Collins, B. A.; Li, Z.; Tumbleston, J. R.; Gann, E.; McNeill, C. R.; Ade, H. *Adv. Energy Mater.* **2013**, *3*, 65.

DOI: 10.1021/jacs.6b02004
J. Am. Chem. Soc. 2016, 138, 4955−4961